ORIGINAL RESEARCH

Numerical Investigation of the Effect of Concrete Injection on the Concrete Joints of the Arched Dam, Under the Applied Stresses

Mansourghanaei M. H.[*1], Mardookhpour A. R.[2]

Abstract

Investigating the safety of dams is of great importance given their critical role in the industry and economy of countries and the catastrophic consequences of their failure. Hence, the present paper examines the impact of incomplete contraction joint injection in the Karun 4 double-curvature arch dam as a case study. In this article, the Abaqus 6.12 finite element software was used to model and analyze 3 numerical models of the Karun 4 dam. These models consist of a linear, integrated, and homogeneous model and two nonlinear models considering the nonlinear behavior resulting from two different types of common contraction joints in the dam's body. The results indicated that a lack of injection led to a significant increase in the maximum principal stresses (MPa) at the upstream section of the dam, such that a large part of this section, which originally worked under compression, is now under tension. The tensile stresses at the upstream abutment and the downstream crest also increased. Moreover, a lack of injection considerably increased the vertical compressive stresses between the contact surfaces (μ). These stresses were increased almost twofold near the injection stop level such that the stresses between monolith zero and one increased from a maximum of 5.13 under complete injection to 11.3. According to the results, with an increase in the joint thickness under the absence of joint injection, considerable amounts (of stress) are added to the maximum principal stresses, minimum principal stresses, dam displacement, and the vertical compressive force between the contact surfaces.

Keywords: Lack of Injection, Joint Thickness, Stress, Arch Dam, Contraction Joint.

✉*Corresponding Author Email: Mhm.Ghanaei@iauc.ac.ir
[1] Ph.D. in Civil, Department of Civil Engineering, Chalous Branch, Islamic Azad University, Chalous, Iran.
[2]Department of Civil Engineering, Lahijan Branch, Islamic Azad University, Lahijan, Iran.

1. Introduction

Providing safety in dams against incoming stresses has always been important [1-3]. On the other hand, the presence of joints in concrete dams has always been a major challenge for researchers [4-6]. In this regard, Existence of tensile stresses in concrete dams can have destructive effects on the dam structure [7-10]. also, not injecting concrete in the structural seams of concrete dams may increase compressive stresses perpendicular to the contact surface [11-14]. Abaqus finite element software is one of the most powerful software for modeling and analyzing concrete dams [15]. The issue of water, which is a basic human need, has become more sensitive with the rise in population and the necessity of agricultural and industrial growth on the one hand and the scarcity of water resources and reservoirs on the other hand. Hence, water shortage is expected to become the primary concern of countries, especially those with arid and semi-arid climates, in the near future. Furthermore, the fluctuations in water flow in rivers, the need for storing water during wet days for use during dry days, and the need for the potential energy of water to produce electricity have made it necessary to build barriers, called dams, across watercourses [16]. Arch dams are special in terms of design technology and require continuous safety evaluations due to the grave consequences of their potential failure. Chooban et al. (2009) employed the finite element method in Abaqus to analyze the Dagonghsan dam, standing 210 m tall, using two different foundation models with and without considering mass and with viscous spring constraints to consider wave energy dissipation. They concluded that the maximum tensile stresses and crest displacement had increased by 10%-25% in the nonlinear analysis compared to the linear analysis due to the slight free-up of the arch. Considering the foundation's mass with viscous springs reduced the tensile stresses and the maximum displacement of the crest in both the linear and nonlinear

models by 5% compared to the massless foundation model [17]. Yao et al. (2012) investigated the seismic response of a 305-m-tall arch dam via Abaqus. They used 8-node hexahedral elements to model the foundation and the dam. According to their results, an increase in the maximum seismic acceleration at a given record increased the sliding and opening of the joints. However, the maximum sliding and opening did not occur simultaneously and were independent [18]. Hariri Ardabili et al. (2013) studied the nonlinear seismic behavior of arch dams at various operation levels by considering the contraction and perimetral joints This research investigated the Dez double-curvature arch dam, with a height of 203 m, as the study case. The loads exerted on the dam were considered to be its weight and the dynamics excitations of the dam-reservoir-foundation combination during the Tabas Earthquake. The joints modeled using node-to-node contact elements were able to open and close and move tangentially. An examination of the results showed that the safety of the dam against a potential earthquake increases with a rise in the level of water in the reservoir [19]. Fersdowsi et al. (2011) investigated the influence of discontinuities in the stone sections of the abutment and the appropriate boundary conditions on the behavior of the Karun 4 dam using Ansys finite element software. In this study, the foundation was modeled with mass and the nonlinear behavior of the stone and concrete were taken into account. The result indicated that considering the discontinuities in the stone remarkably affects the stress distribution in the dam body and produces a better evaluation of the dam behavior [20]. Ahmadi and Ahmadi (2012) conducted an analysis of the malpasset arch dam by taking into consideration the nonlinear geometric behavior of the material under the force of the weight and hydrostatic pressure up to the crest level. Two layers of 20-node nonlinear elements were used to mesh the dam body. The results indicated a rise in the

maximum displacement with a reduction in the joint parameters. The responses were closer at lower displacements, but differences in the criteria were observed as the displacements increased. The plasticity models utilized produced larger fracture mechanics responses in general [21]. The present study examines the effect of incomplete injection in the contraction joint of the Karun 4 double-curvature arch dam. The Abaqus 6.12 finite element software was employed for the numerical simulations. The present article introduces the software and the modeling procedure in addition to explaining the application of the loads and the contact boundary conditions at the joints. Finally, the numerical results are validated.

2. Materials and Methods
2.1. Specifications of the Karun 4 Dam

The Karun 4 dam is located in southwestern Iran on the river Karun immediately upstream from the intersection of the Monj and Karun rivers. The river bed is 840 m above sea level and has a width between 30 m and 60 m. The valley where the dam is built has an asymmetric V shape with a generally steeper slope on the left side and a crest-level width of about 350 m. Accordingly, the width-to-height ratio of the value is 1:8, which is ideal for an arch dam. The following tables represent the specifications of the Karun 4 dam [22].

Table 1. Dam Body Parameter

Parameter	Value	Parameter	Value
Dam Type	Double-Curvature Arch Dam	Width at the Foundation	37-52 m
Height From the Foundation	230 m	Height from the Floor	190 m
Crest Length	440 m	Total Concrete Volume	62 million m^3
Crest Width	7 m	Crest-Level Valley Width	350 m

Table 2. Dam Reservoir Parameters at the 1.25 Level

| Parameter	Value
Total Reservoir Volume	2190 million m^3
Reservoir Surface Area	29 km^2
Lake Length	41 km Along the Armand Branch and 28 km Along the Bazft Branch
Lake Width	Variable

Table 3. Reservoir Water Levels (Measured from the Sea Level)

Parameter	Value	Parameter	Value
Normal Level	1025	Sediment Elevation	870
Minimum Operation Level	996	Normal Tailwater Level	845
Probable Maximum Flood (PMF) Water Level	1033.3	Probable Maximum Flooding (PMF) Tailwater Level	860

2.2. Finite Element Model

The Karun 4 dam model was meshed using 3852 linear 8-node cubic elements. The largest and smallest element dimensions were 16.5 m and 5.3 m. Moreover, two different element types were used since two different analyses, namely thermal and static, were performed. The DC3D8 element was used for the thermal analysis, and the C3D8R element was employed for the stress-strain analysis. These elements differ in their respective formulations. In this model, the foundation was considered rigid and the materials were assumed to behave nonlinearly. The meshed dam model, consisting of 22 separate monolith and 21 contraction joints, is displayed in the figure below.
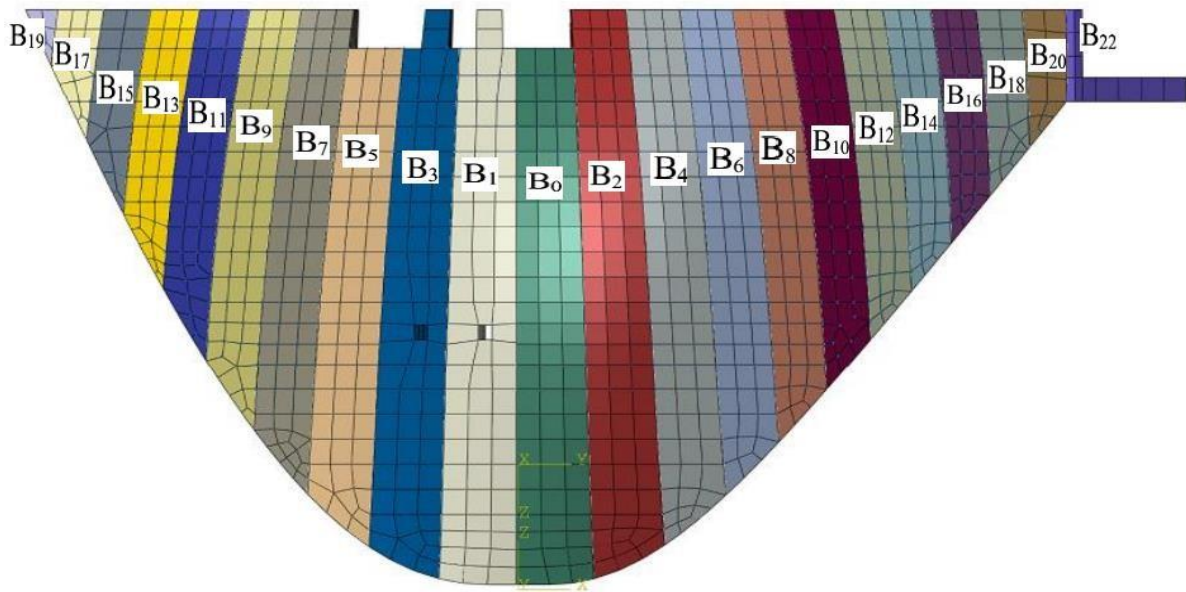
Figure 1. The Finite Element Model of the Karun 4 Dam

By reviewing the technical literature that has been done in the field of nonlinear analysis of arched concrete dams by considering contraction joints, it can be seen that in these studies, the joint parameters are uniformly distributed among all the blocks in the height of the dam. In this regard, the following assumptions have been considered for this research:

1) The non-linear behavior of the body except for the location of the seams has been neglected.

2) The incoming loads from the reservoir upstream of the hydrostatic dam are considered.

3) The investigation of the problem will be against static loads.

4) The geometric model related to the Karun 4 dam available in reference [23] has been used.

5) The foundation of the dam is assumed to be rigid.

2.3. Loading

The load due to the weight of the dam, that due to the reservoir, and a thermal load were considered as the loads exerted to the dam. The one-time exertion of the weight to the integrated analytical model causes the dam body to hang from the supports and, hence, high tensile stresses to be created in the model of the dam body, especially in the upper sections, almost parallel to the surface of the foundation or the horizon. These stresses are absent in reality due to the presence of contraction joints in the dam body and the gradual concrete placement for the monolith in it. Thus, the weight load was applied in different stages. For stepwise modeling of the dam, the key editing tool was used in Abaqus to eliminate the stiffness of the upper section at each step of the gravitational loading. Moreover, the weight loading was performed in 5 static models with 3, 4, 6, and 12 loading steps in order to ensure the validity of the stepwise loading. It was observed that the model with 6 loading steps had a suitable number of elements in addition to good stress conditions at the abutments [23].
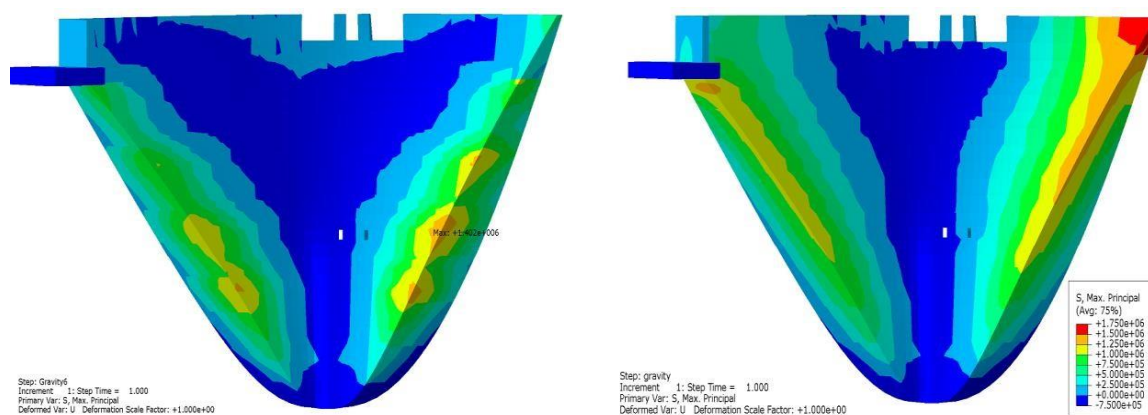
Figure 2. Maximum Principal Stresses (MPa): (a) Single-Step Loading and (2) 6-Step Loading

Fig. 2 displays the difference between the maximum principal tensile stresses under two weight loading conditions. As can be seen, the one-time application of the weight load increases the maximum principal tensile stresses parallel to the foundation at the abutments, especially at the top of the dam. However, a stepwise application of the weight reduces the tensile stresses at the foundation, especially at its upper section. In order for a thermal analysis to be performed on the dam, the existing temperatures were assigned as the boundary conditions to the nodes on the dam body. Then, the DC3D8 thermal element was used to perform a thermal analysis. This analysis determined the temperatures of all the nodes in the dam, which were then applied as secondary temperatures to the static analyses. The initial (injection) temperature of the dam was assumed to be 17°C. It must be noted that the thermal and stress-strain analyses must have identical meshes.

3. Analysis and Results

This section concerns the results of the numerical model. Three different numerical models were analyzed using Abaqus: one linear model that considers the dam body as integrated and without joints and two nonlinear models that consider contraction joints in the dam body. One of the nonlinear models assumes the joints to be smooth (in the absence of shear keys), and the other assumes the joints to be rough (in the presence of shear keys in the joints). To determine the effect of the increase in the initial thickness on the behavior of the dam under the absence of injection, we analyzed the smooth joint and compared the results to previous works.

3.1. Validation of the Model

In order to ensure the validity of the numerical results, we conducted 4 static analyses with two different reservoir levels according to Table 4 and compared the results to the dam monitoring results in [24] and the complementary analysis reports in [22]. The displacement results at monolith 0, 9, and 10, which represent the center, left, and right monolith, respectively, in the dam body, were derived in Analyses 2, 3, and 4, respectively, and were compared to the dam monitoring results. The following figure represents the dam displacements in the mentioned monolith. A review of the graphs in Fig. 3 indicates that the nonlinear analysis results better agreed with the measurements compared to the linear analysis results. This shows that modeling the contraction joints has improved the accuracy of the dam's behavior. Moreover, since the nonlinear analysis results are similar, one may conclude that the values selected for the joint parameters in both the smooth and rough models were appropriate and that the model is valid.

Table 4. Validation Analyses

Thermal Load	Analysis Procedure		Weight Load	Analysis Type	Water Level	Analysis Number
	Reservoir Load					
Winter	All Hydrostatic Loads		6 Steps	Linear Elastic (Li)	3.1033	1
Winter	Without Sediment		6 Steps	Linear Elastic (lns)	99.1023	2
Winter	Without Sediment		6 Steps	Nonlinear with Smooth Joints (NL-S)	99.1023	3
Winter	Without Sediment		6 Steps	Nonlinear with Rough Joints (NL-R)	99.1023	4
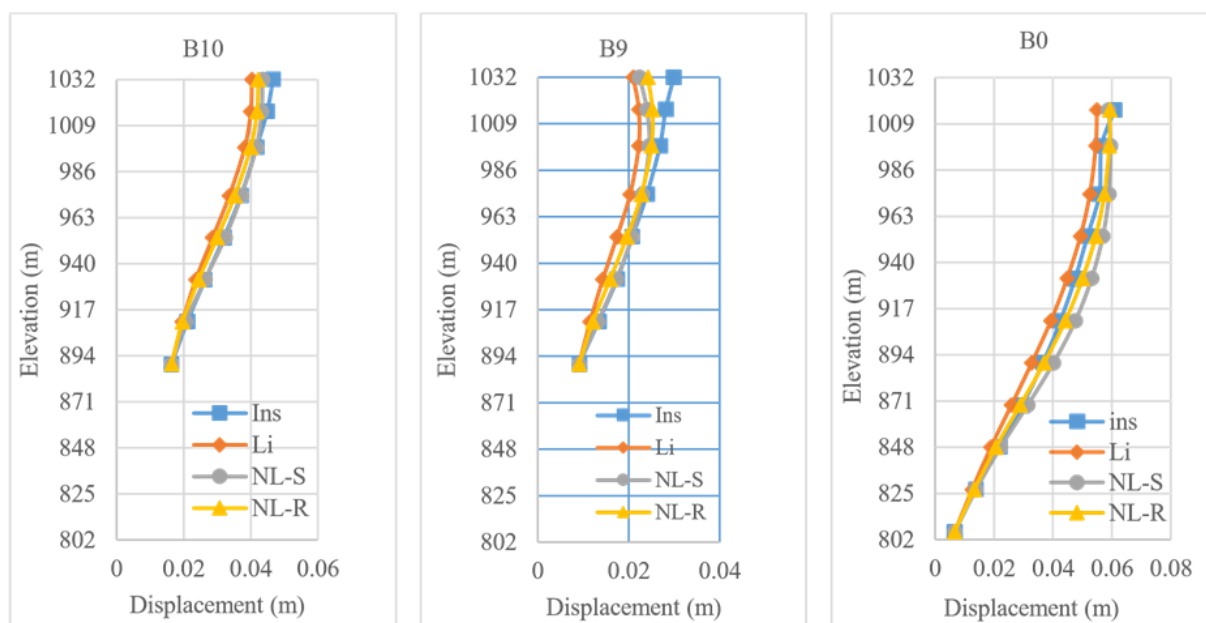
Figure 3. The Graph of Displacements at Monolith 1, 9, and 11 in the Analyses and those Obtained from Instrument Measurements

6
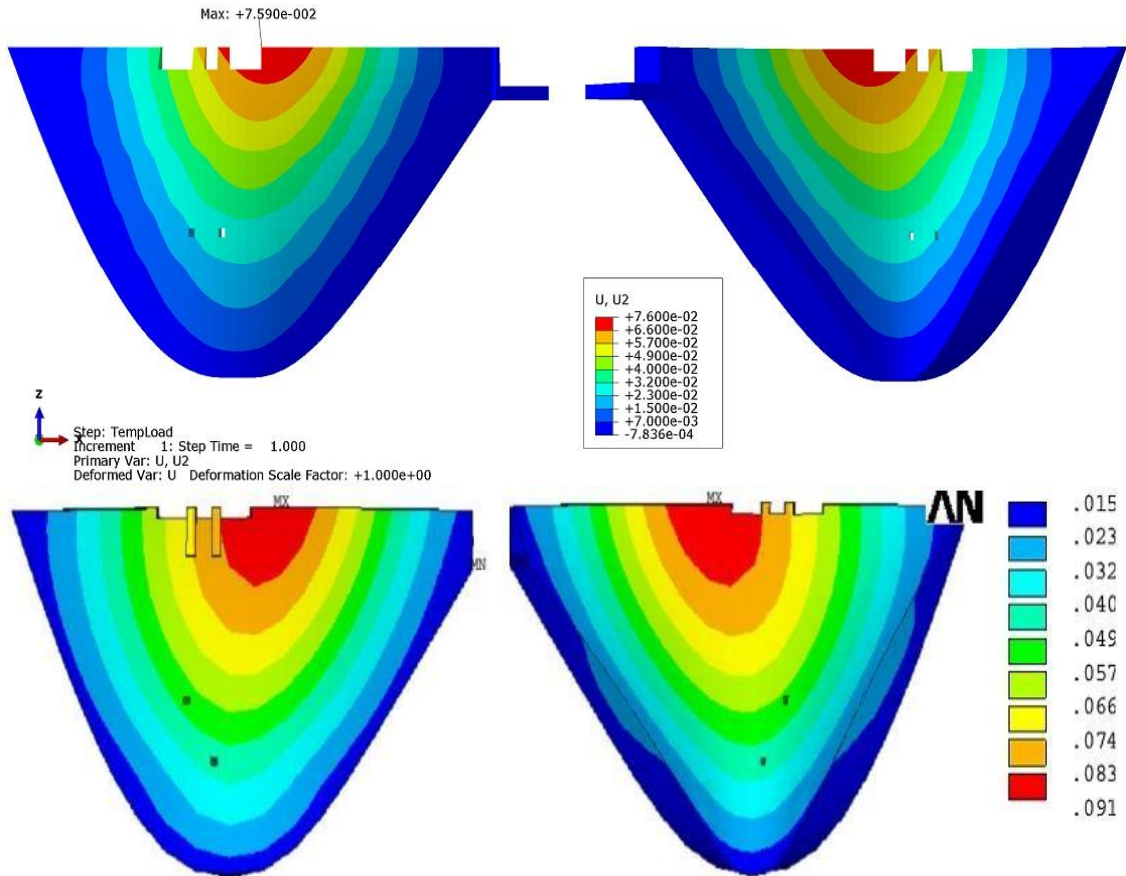
Figure 4. Displacements in the Dam Body at the 1033.3 level: (a) Linear Analysis and (b) Complementary Analysis Reports of the Dam Body and Abutments

As shown in the figure, the displacement distributions are similar in the two models. However, the displacement in the linear model is smaller than that in the final step of the dam study. As mentioned previously, this is due to the rigidity of the foundation in the numerical model. The addition of a foundation movement of 1.115 m to the numerical model results in very similar displacements especially at the crest, indicating the appropriateness of the dam's model.

3.2. The Effect of the Absence of Injection on the Opening of the Contraction Joints

The effects of the contraction joints were considered by placing adjacent monolith at a distance of 3 mm from each other and, then, applying the vertical contact pressure relationship to them. The 3 mm distance is the initial distance between the joint surfaces. If the distance increases beyond 3 mm after loading, the opening of the joint is considered, and if the distance reduces to less than 3 mm, the closing of the joint is considered. For an investigation of the effect of an absence of injection on the opening of the contraction joints, the following figures display the opening of the joint surfaces under full injection and a lack of injection with winter-time thermal loading. Given that the opening is unknown between monolith 0 and 1 in the left figure, it is shown separately in the right figure.
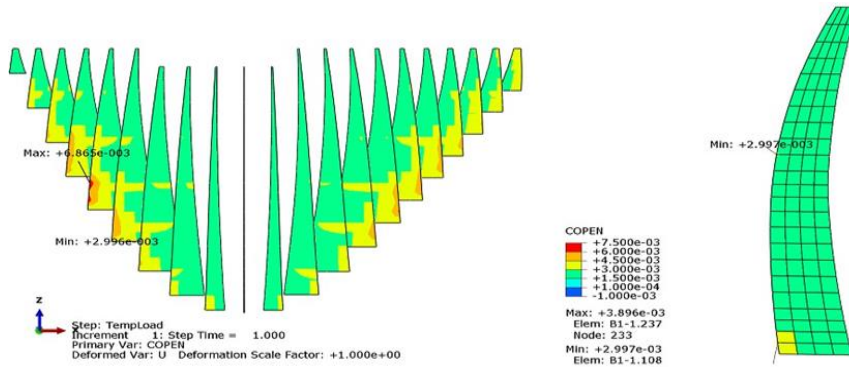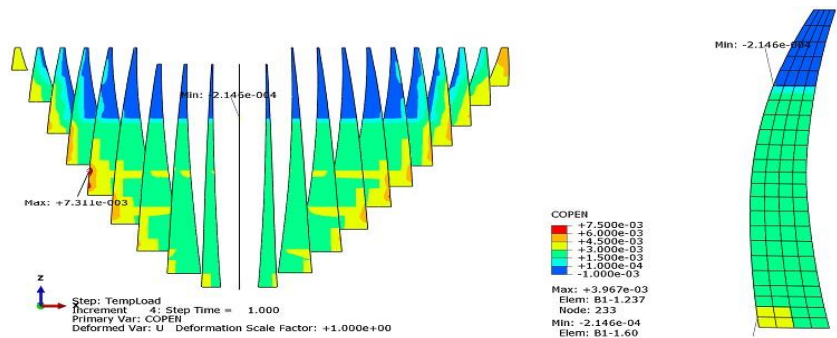
Figure 5. Joint Opening in m at a Normal Level and Under Winter-Time Thermal Loading in the Nonlinear Analysis and with Full Injection in the Smooth Joint with a Friction Coefficient of 1
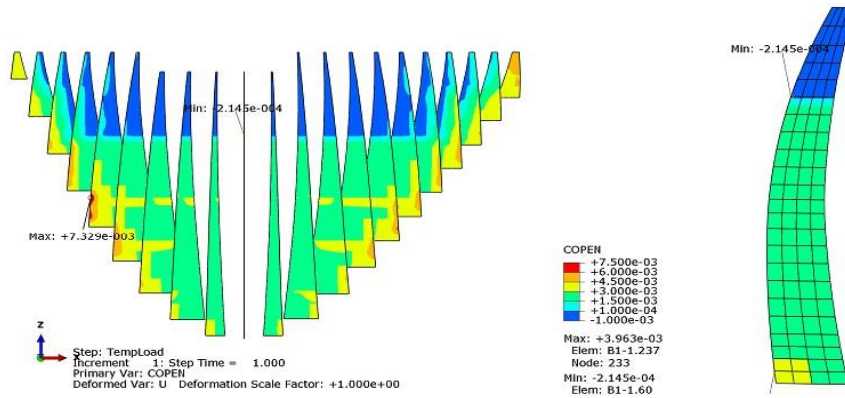
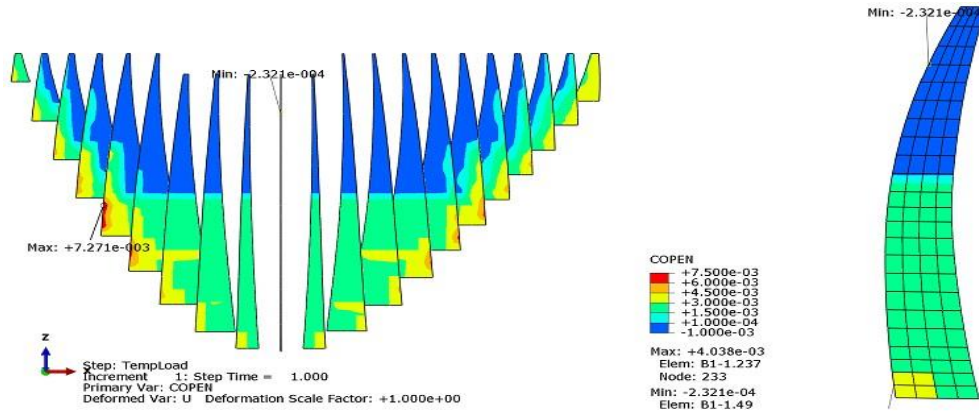**(A) A Friction Coefficient of 1**
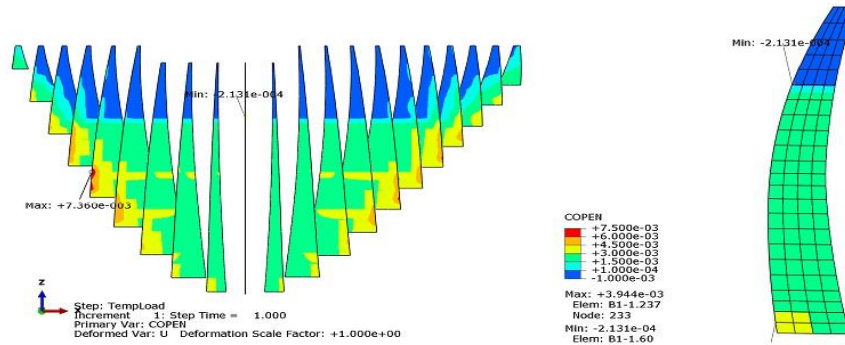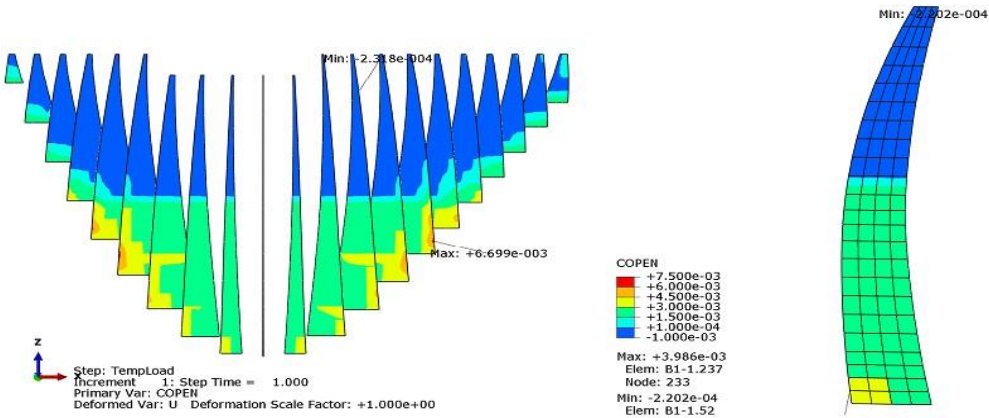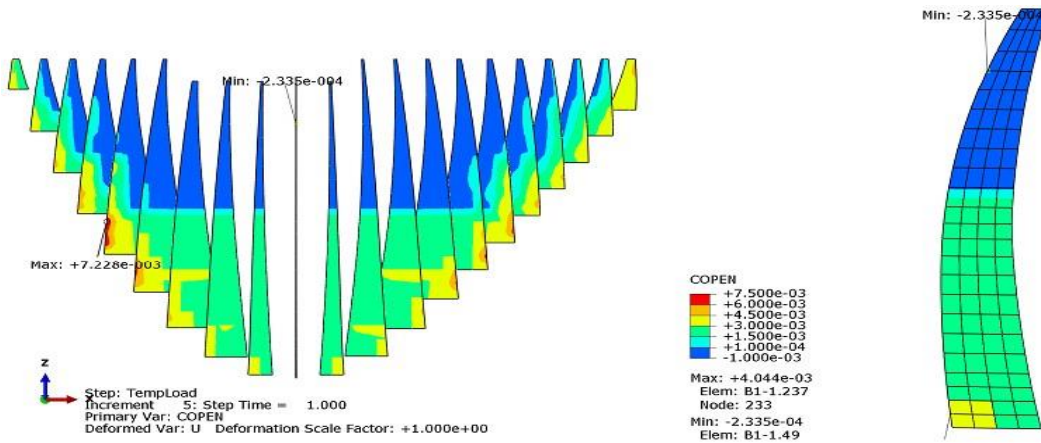

(B) A Friction Coefficient of 0
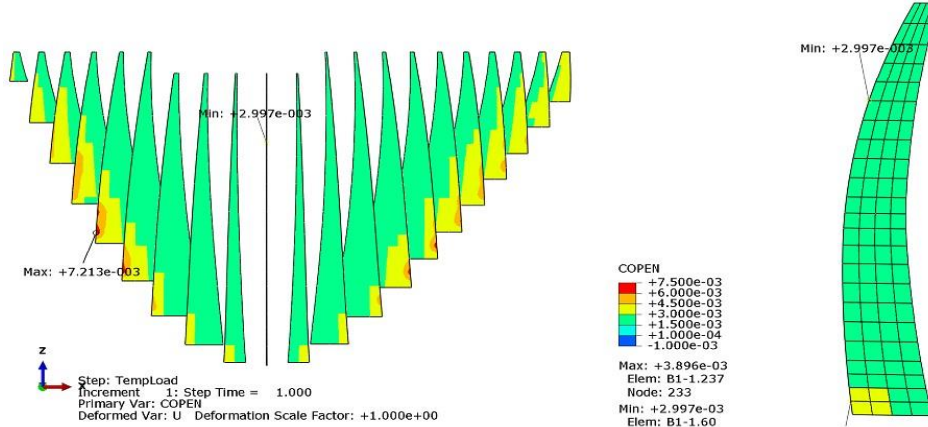

(C) A Friction Coefficient of 10

Figure 6. Joint Opening in m at a Normal Level and Under Winter-Time Thermal Loading in the Nonlinear Analysis and with no Injection from a Level of 955 m Upward in the Smooth Joint with Various Friction Coefficients

8

(A) A Friction Coefficient of 1

(B) A Friction Coefficient of 0

(C) A Friction Coefficient of 10

Figure 7. Joint Opening in m at a Normal Level and Under Winter-Time Thermal Loading in the Nonlinear Analysis and with no Injection from a Level of 915 m Upward in the Smooth Joint with Various Friction Coefficients

As shown in Fig. 5, the joints have opened near the upstream abutment under full injection Since the dam moves downstream under the loads, the upstream monolith near the abutment undergo tension and experience deformation at their upstream faces with a reduction in thickness.

Furthermore, the dam displacements show that the dam exhibits negative deformation in regions with joint opening, indicating block torsion in these regions. Hence, the joint opening near the abutment can be attributed to these two phenomena, namely the shortening and torsion of the monolith

9

at the upstream face. In addition, given that the analysis was performed under winter-time thermal loading, one may conclude that this loading contributes to the opening of the joints due to a reduction in temperature and the shrinking of the monolith. The decrease in the friction coefficient from 1 to 0, shown in Fig. 8, reduced the joint opening at the end monolith owing to the further movement of the monolith downstream. As the friction coefficient increased from 1 to 10, no significant difference was observed in the joint opening distribution. The following figures display the joint opening when the shear key was (rough joint) used.

Figure 8. Joint Opening in m at a Normal Level and Under Winter-Time Thermal Loading in the Nonlinear Analysis and with Full Injection in the Rough Joint
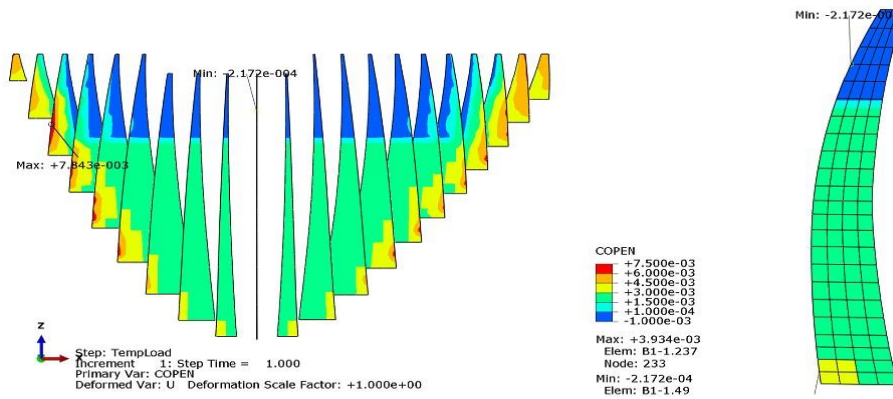
Figure 9. Joint Opening in m at a Normal Level and Under Winter-Time Thermal Loading in the Nonlinear Analysis and with no Injection in the Rough Joint from a Level of 955 m Upward
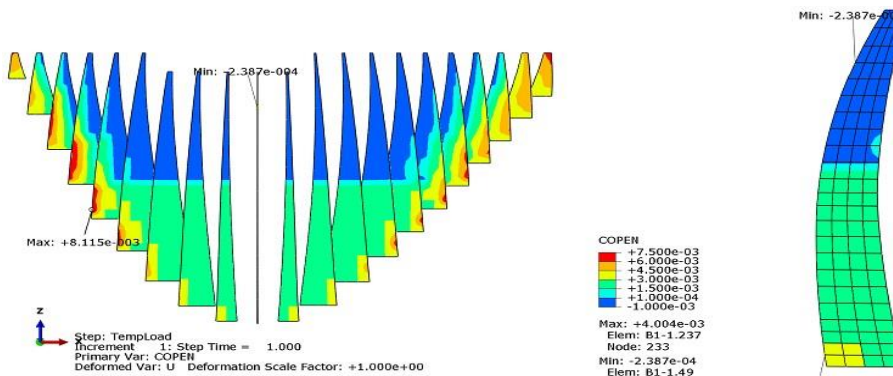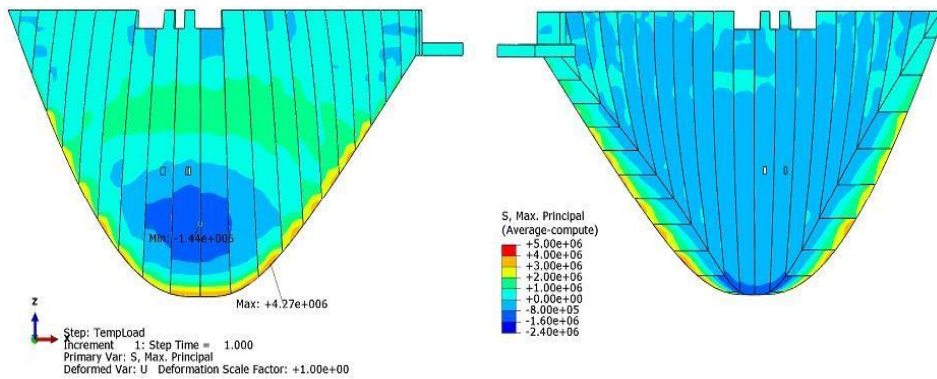

Figure 10. Joint Opening in m at a Normal Level and Under Winter-Time Thermal Loading in the Nonlinear Analysis and with no Injection in the Rough Joint from a Level of 915 m Upward

10

As seen in the figures, the changes in the opening of the joints in case of no injection in the rough joint (shown in Figs. 8-10) are similar to those for the smooth joint (Figs. 5-7). However, the maximum opening in this case is larger than that in the case of the smooth joint. Moreover, the results indicate that the maximum opening occurs near the left abutment, and the openings on the left side are generally larger than those on the right side. In addition, the regions with a maximum opening under the rough joint case are mostly at the upper levels of the dam (under maximum injection heights of 915 m and 955 m).

3.3. The Effect of an Increase in the Initial Joint Thickness on the Behavior of the Dam with the Absence of Injection

For the impact of the initial joint thickness on the dam's behavior to be determined in case of no injection, we increased the distances between the contact surfaces beyond 3 mm. However, the rest of the joint parameters (the friction between the joint surfaces, the vertical compressive force defined between the adjacent monolith, and the collision between the adjacent monolith at a distance of 1.1 mm in the regions without injection) were kept constant. As a result, no difference occurred between the stresses and displacement of the dam in the case of the full injection in the contraction joints. These analyses were performed as examples and solely for joints without shear keys and with a friction coefficient of 1 and an increase in the joint thickness to 5 mm and 1 cm at the 915 m and 955 m levels. The figures below demonstrate the distribution of the maximum principal stresses under a maximum injection height of 955 m.
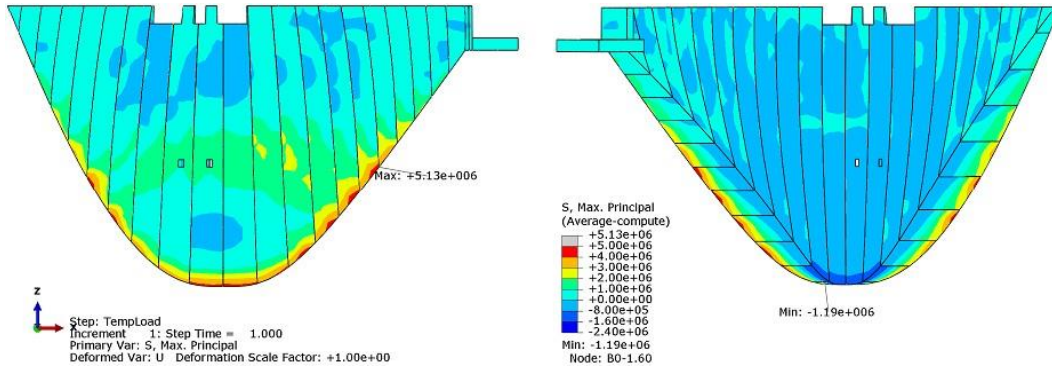

(A) A Joint Thickness of 5 mm
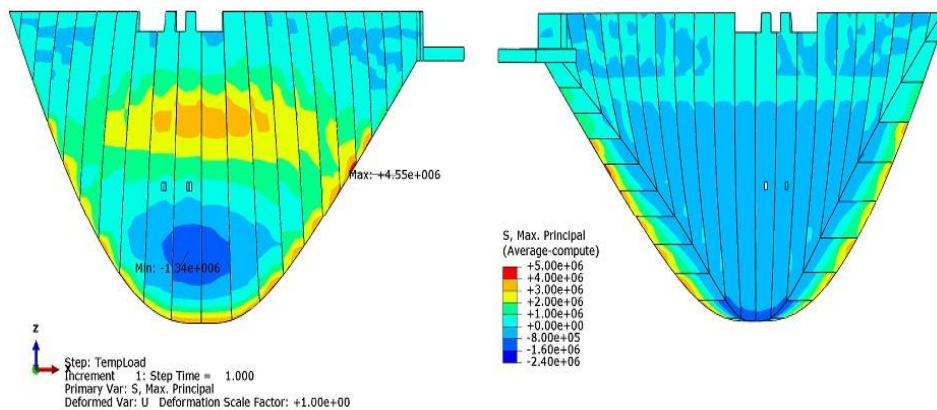
(B) A Joint Thickness of 1 cm

Figure 11. The Maximum Principal Stress Distribution at the Upstream and Downstream of the Dam in Pa at a Normal Level and Under Winter-Time Thermal Loading in the Nonlinear Analysis and with no Injection from a Level of 955 m Upward in the Smooth Joint with a Friction Coefficient of 1 and Various Joint Thicknesses
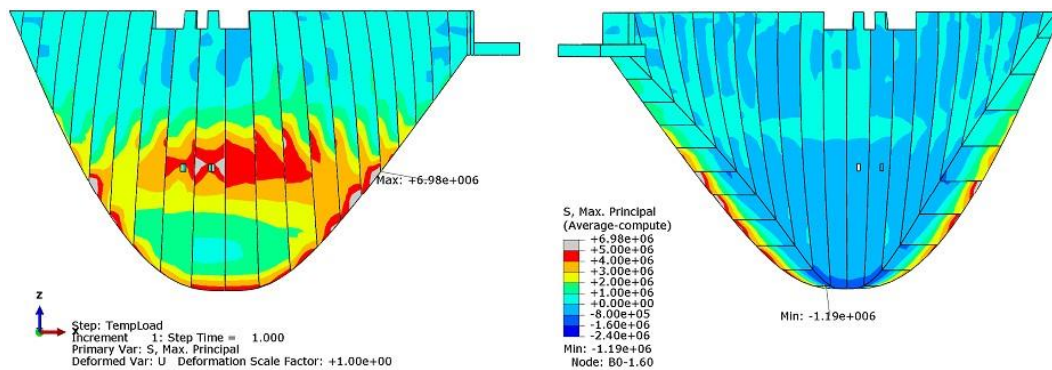
As shown in the above figures, an increase in the joint thickness to 5 mm increased the tensile stresses in the dam's body compared to the 3 mm thickness. A further increase to 1 cm increases the tensile stresses in the dam body near the injection location beyond 3 MPa, while this value is only 2 MPa for a thickness of 5 mm and less than 1 MPa for a thickness of 3 mm.

The distribution of the maximum principal stresses is shown in the figure below for a study of the impact of a rise in the no-injection height under an increase in the initial thickness of the joint.
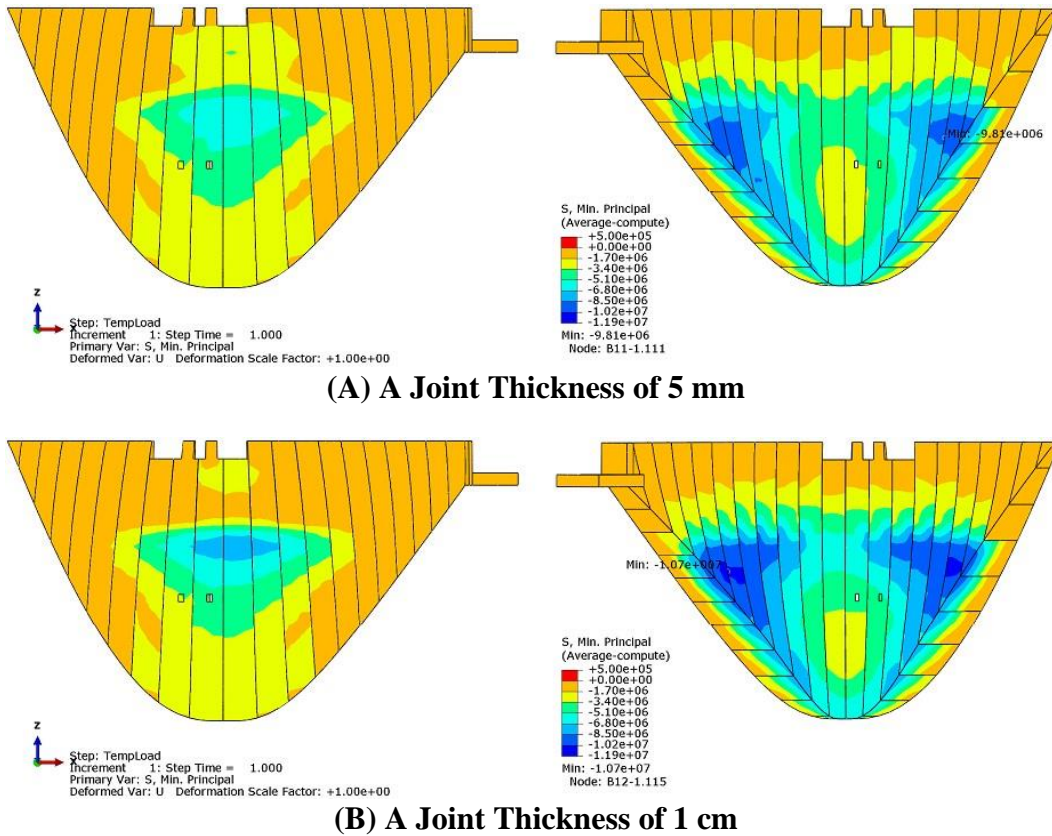

(A) A Joint Thickness of 5 mm

(B) A Joint Thickness of 1 cm

Figure 12. The Maximum Principal Stress Distribution at the Upstream and Downstream of the Dam in Pa at a Normal Level and Under Winter-Time Thermal Loading in the Nonlinear Analysis and with no Injection from a Level of 915 m Upward in the Smooth Joint with a Friction Coefficient of 1 and Various Joint Thicknesses

As shown in the above figure, a rise in the no-injection height increased the tensile stresses in the dam's body compared to the case with a maximum injection height of 955 m (Fig. 9), such that the almost upstream face of the dam is under tension. This increase in stress has exceeded 5 MPa at a joint thickness of 1 cm near the injection location. These results indicate that, in case of no injection in the joints in a double-curvature dam with a relatively low initial thickness of the joints (about 3 mm in these studies), the dam design in the regions with no injection (or incomplete injection) act as a horizontal curve by moving downstream under the applied hydrostatic loads. This action takes part in the transfer of the loads with a small delay. The delay in the formation of the horizontal curve action slightly affects the stress distribution while significantly influencing the deformations in the dam. The minimum principal stress distribution is shown in the following figure for a study of the impact of the increase in the initial joint thickness on the compressive stress in the dam.

12

(A) A Joint Thickness of 5 mm
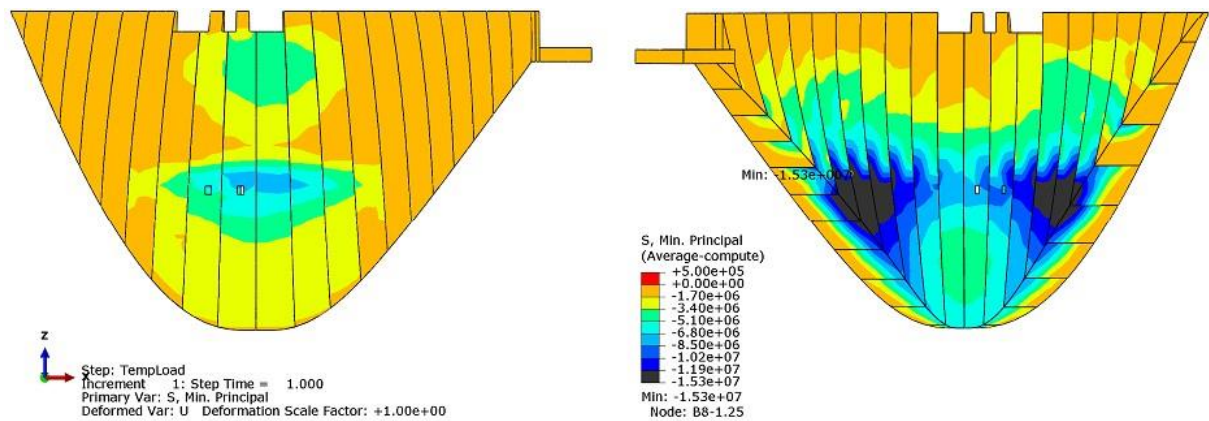

(B) A Joint Thickness of 1 cm

Figure 13. The Minimum Principal Stress Distribution at the Upstream and Downstream of the Dam in Pa at a Normal Level and Under Winter-Time Thermal Loading in the Nonlinear Analysis and with no Injection from a Level of 955 m Upward in the Smooth Joint with a Friction Coefficient of 1 and Various Joint Thicknesses

According to the figure, an increase in the initial joint thickness reduced the compressive stresses at the upstream and downstream crests of the dam. Nevertheless, the compressive stresses at the upstream and downstream injection locations and at the downstream abutment increased in parallel and lower than the injection location. This increase in compressive stress at a joint thickness of 1 cm was 1.79 MPa higher than that at a joint thickness of 3 mm. As shown in the figure above, with an increase in the no-injection height, the compressive stresses at the upper section of the dam at the upstream and downstream sides increased compared to the case with no injection above 955 m (Fig. 13). Moreover, the compressive stresses at the downstream abutment increased considerably, especially for the dam with a joint thickness of 1 cm. The following figures demonstrate the distribution of displacement in the dam with an increase in the joint thickness. A comparison of the above two figures with displacement results from the nonlinear no-injection analysis without a shear key and with an initial joint thickness of 3 mm indicates that an increase in the initial joint thickness significantly increases the dam displacements. Specifically, in the case with a maximum injection height of 955 m with initial joint thicknesses of 5 mm and 1 cm, the displacement increased by 24% and 68%, respectively. Similarly, the increase corresponding to the case with a maximum injection height of 915 m with initial joint thicknesses of 5 mm and 1 mm were 34% and 111%, respectively. The following figures show the distribution of vertical stress between the joint surfaces for an investigation of the impact of the initial joint thickness on the vertical stresses in the case of a lack of injection.
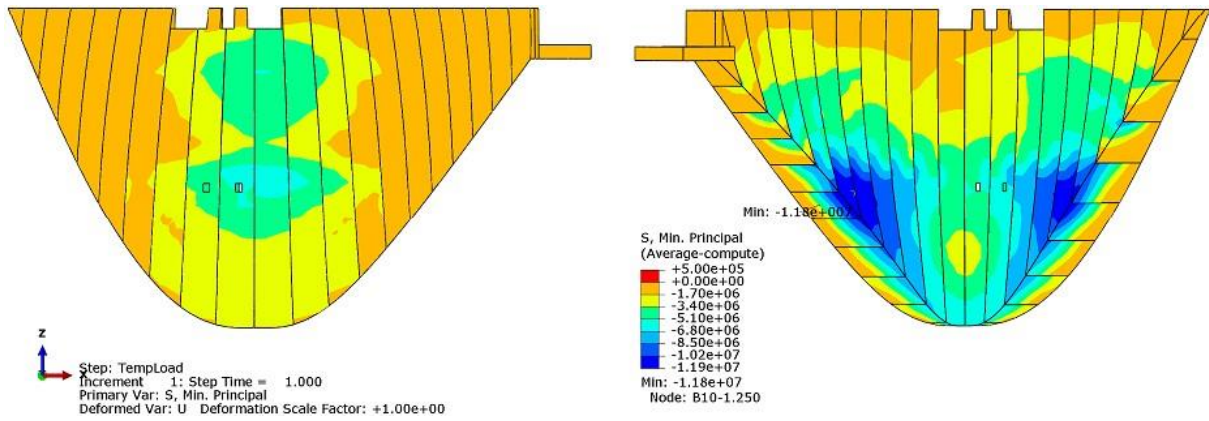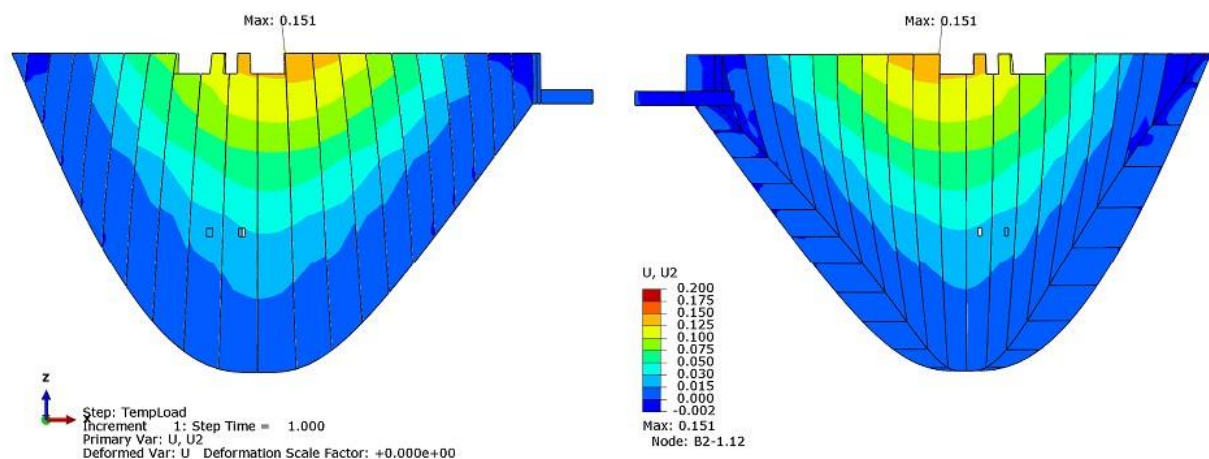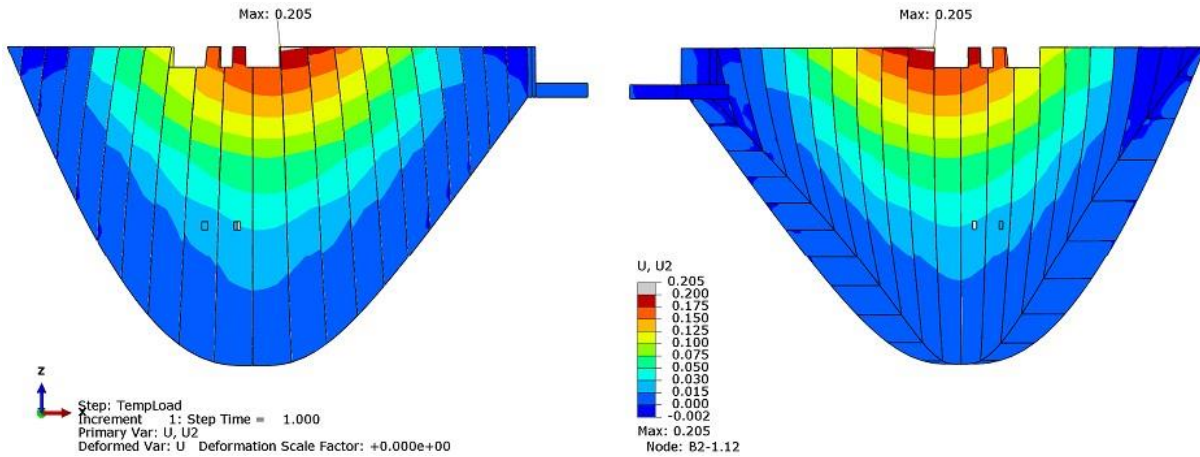
(A) A Joint Thickness of 5 mm

(B) A Joint Thickness of 1 cm

Figure 14. The Minimum Principal Stress Distribution at the Upstream and Downstream of the Dam in Pa at a Normal Level and Under Winter-Time Thermal Loading in the Nonlinear Analysis and with no Injection from a Level of 915 m Upward in the Smooth Joint with a Friction Coefficient of 1 and Various Joint Thicknesses

(A) A Joint Thickness of 5 mm

14

(B) A Joint Thickness of 1 cm

Figure 15. The Distribution of Displacements in m in the Downstream Direction at a Normal Level and Under Winter-Time Thermal Loading in the Nonlinear Analysis and with no Injection from a Level of 955 m Upward in the Smooth Joint with a Friction Coefficient of 1 and Various Joint Thicknesses
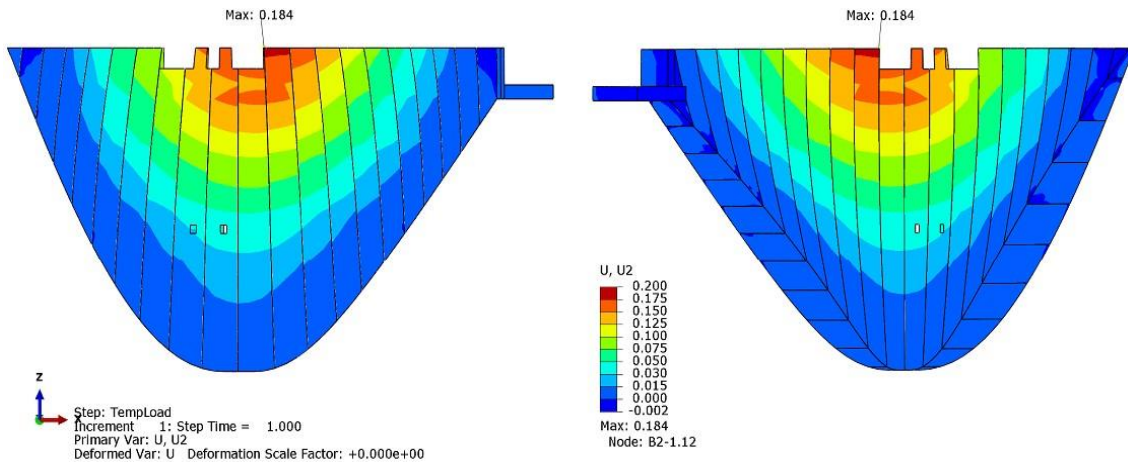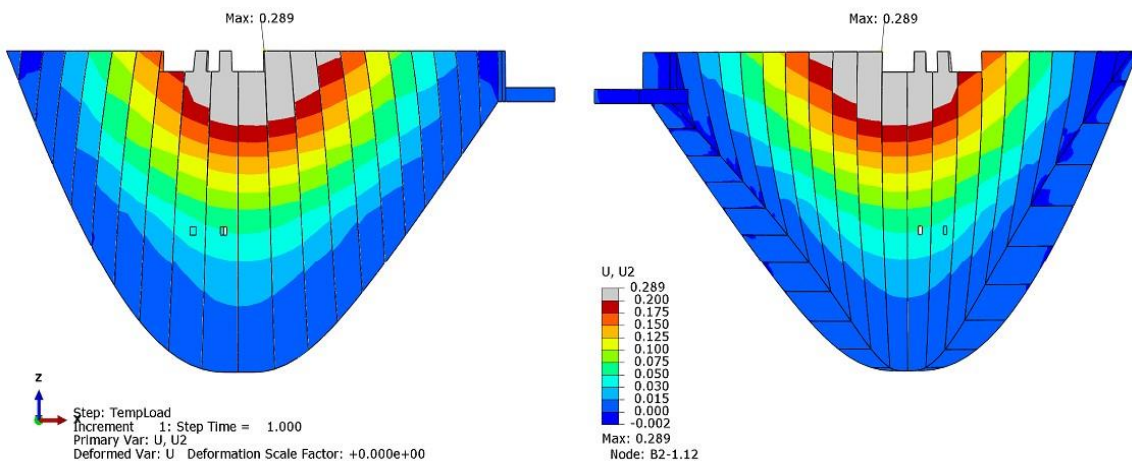
(A) A Joint Thickness of 5 mm

(B) A Joint Thickness of 1 cm

Figure 16. The Distribution of Displacements in m in the Downstream Direction in m at a Normal Level and Under Winter-Time Thermal Loading in the Nonlinear Analysis and with no Injection from a Level of 915 m Upward in the Smooth Joint with a Friction Coefficient of 1 and Various Joint Thicknesses
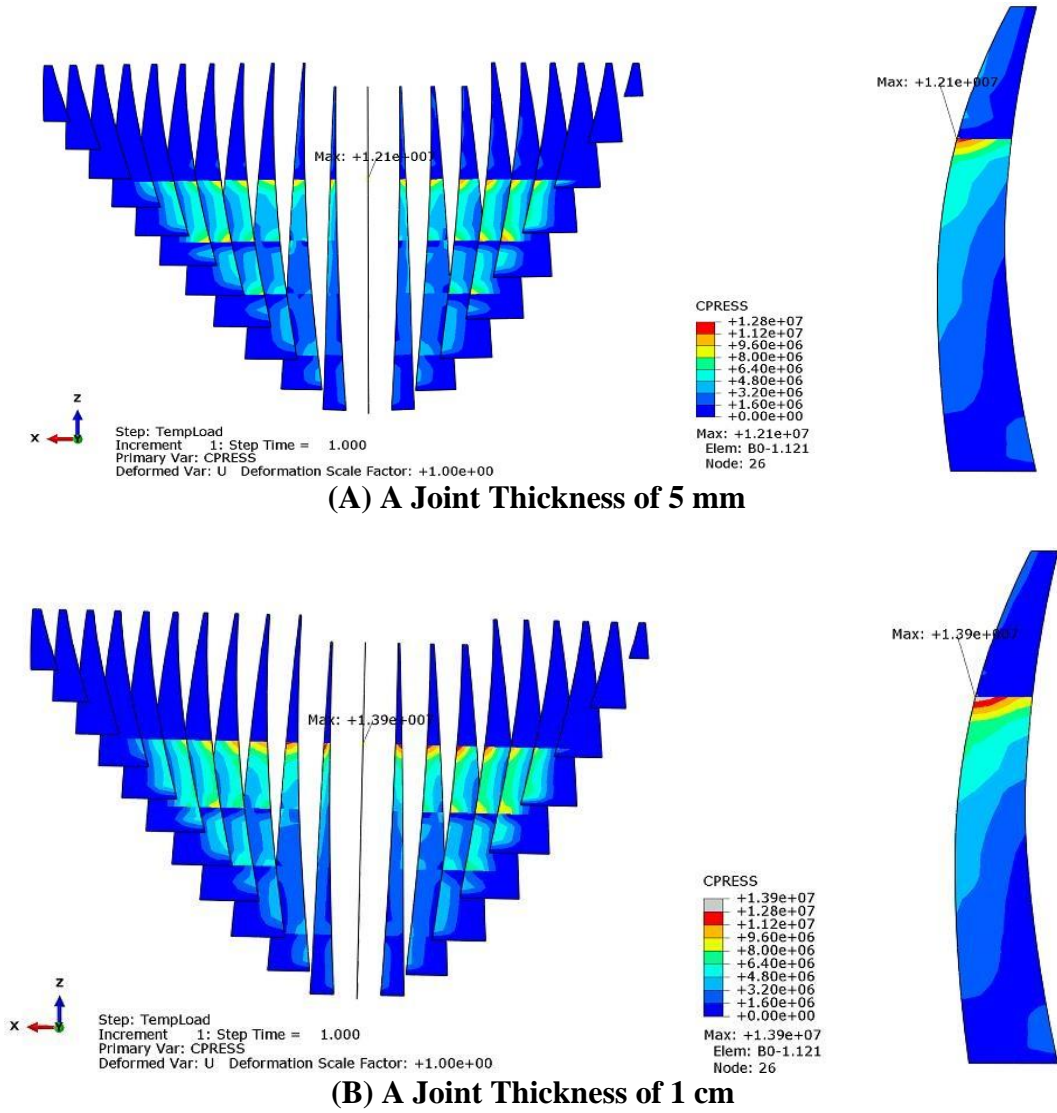
(A) A Joint Thickness of 5 mm

(B) A Joint Thickness of 1 cm

Figure 17. The Distribution of Vertical Compressive Stress on the Contact Surfaces Between the Adjacent Monolith **0 and 1 in Pa at a Normal Level and Under Winter-Time Thermal Loading in the Nonlinear Analysis and with no Injection from a Level of 955 m Upward in the Smooth Joint with a Friction Coefficient of 1 and Various Joint Thicknesses**

According to the above figure, with an increase in the initial thickness in regions with no injection, no contact is created between the joint surfaces, especially for the joint with an initial thickness of 1 cm. Hence, the vertical stresses between the contact surfaces remain 0 or very small unless in the middle monolith mostly in the joints with an initial thickness of 5 mm. It is also observed that the vertical compressive stress in the injected parts, especially at the injection location, is higher compared to the joint with an initial thickness of 3 mm. Specifically, the maximum vertical compressive stress in the joint with an initial thickness of 1 mm increased by 2.6 MPa relative to that in the joint with an initial thickness of 3 mm. The distribution of the vertical stresses between the joint surfaces due to an increase in the no-injection height with initial thicknesses of 5 mm and 1 cm are displayed in the figures below.

16
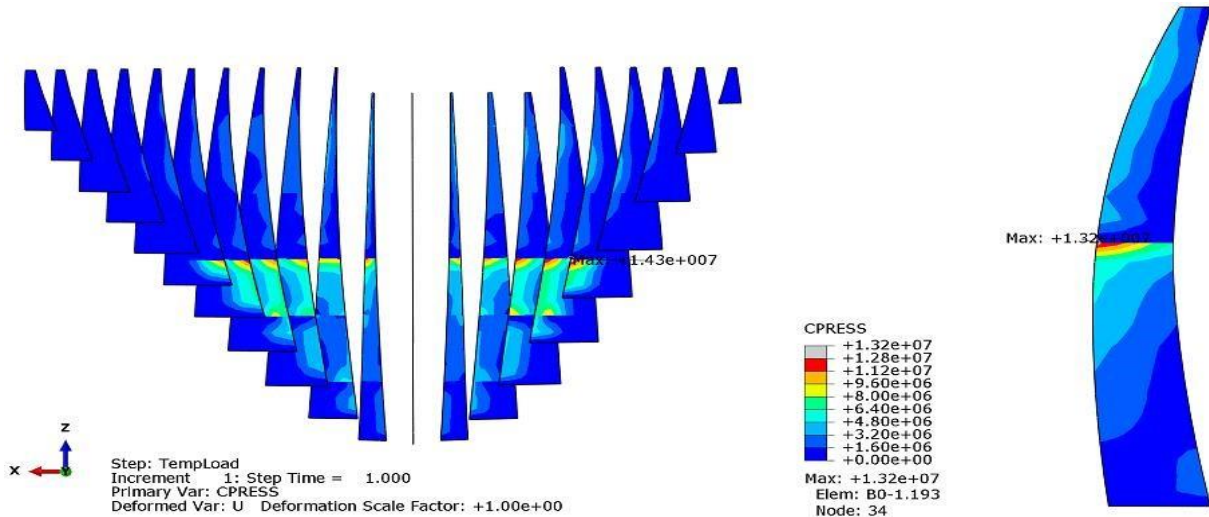
(A) A Joint Thickness of 5 mm
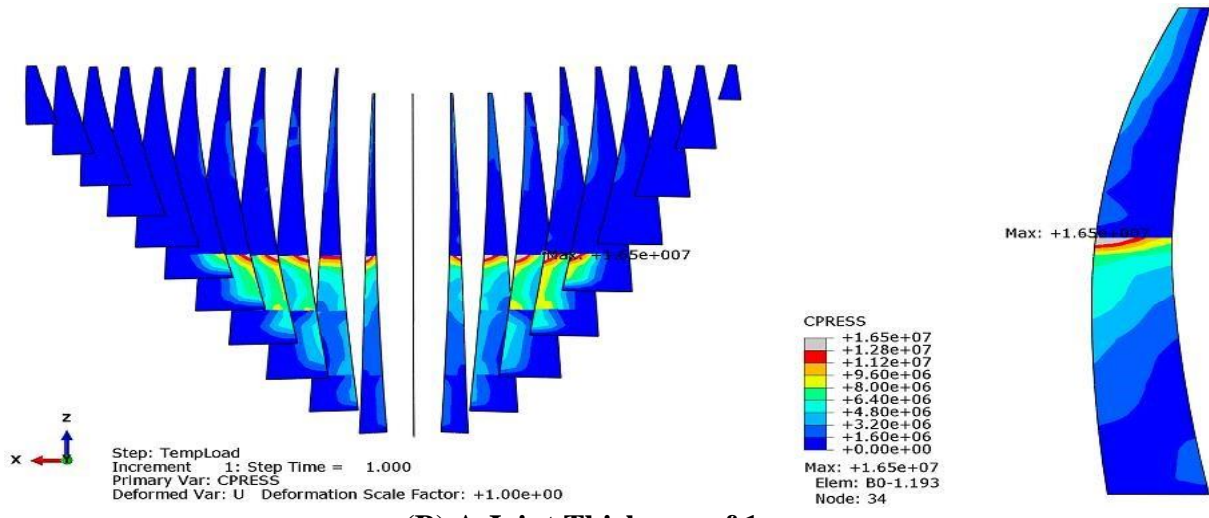

(B) A Joint Thickness of 1 cm

Figure 18. The Distribution of Vertical Compressive Stress on the Contact Surfaces Between the Adjacent Monolith 0 and 1 in Pa at a Normal Level and Under Winter-Time Thermal Loading in the Nonlinear Analysis and with no Injection from a Level of 915 m Upward in the Smooth Joint with a Friction Coefficient of 1 and Various Joint Thicknesses

A comparison between the case with a maximum injection height of 955 m (Fig. 17) and the above figure indicates that a rise in the no-injection height resulted in more contact between the monolith in the regions with no injection along with considerable deformations. Accordingly, the vertical compressive stresses in the regions with injection and at the injection location increased compared to the case with a maximum injection height of 955 m. This rise in stress was 2.6 MPa in the joint with an initial thickness of 1 cm and 1.1 MPa in the joint with an initial thickness of 5 mm. The figures below show the distribution in the joint opening at two different no-injection levels with an increase in the initial joint thickness.

17
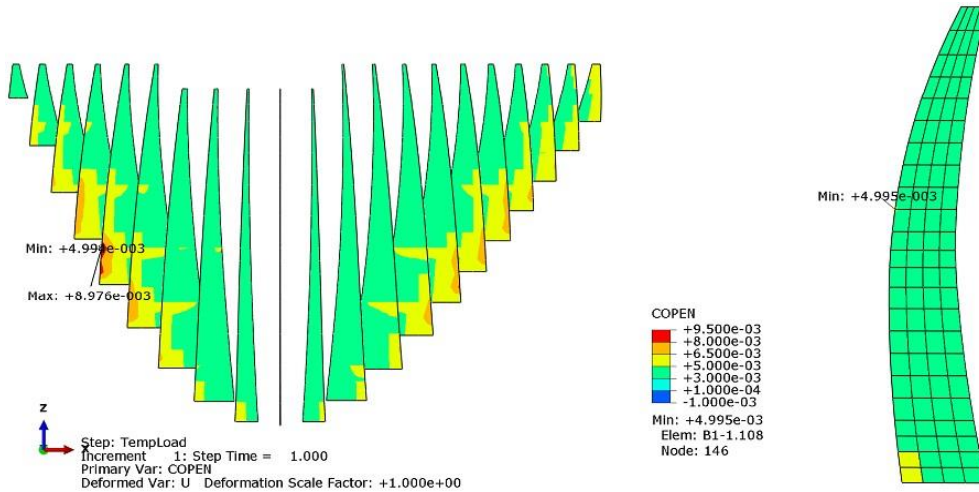
Figure 19. Joint Opening in m at a Normal Level and Under Winter-Time Thermal Loading in the Nonlinear Analysis and with Full Injection in the Smooth Joint with a Joint Thickness of 5 mm
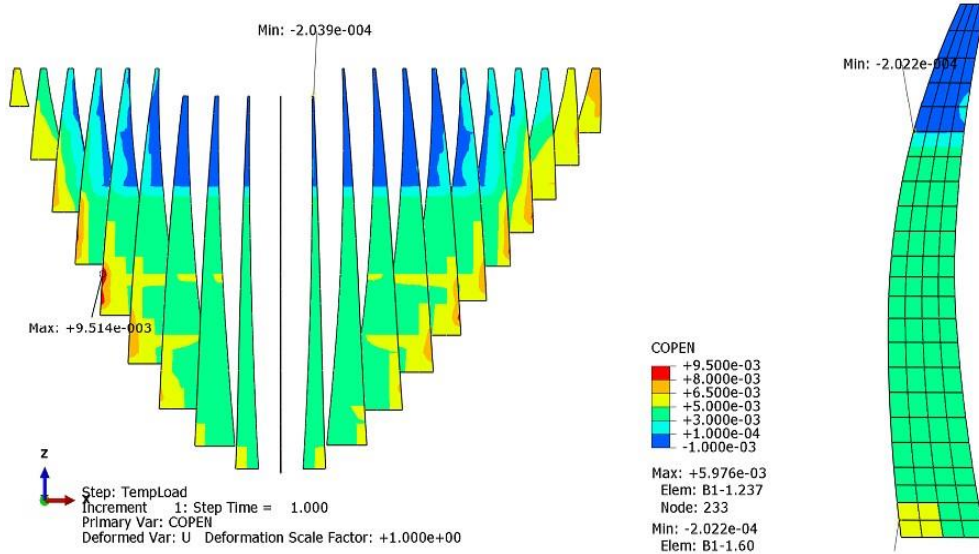
(A) No Injection from a Level of 955 m Upward
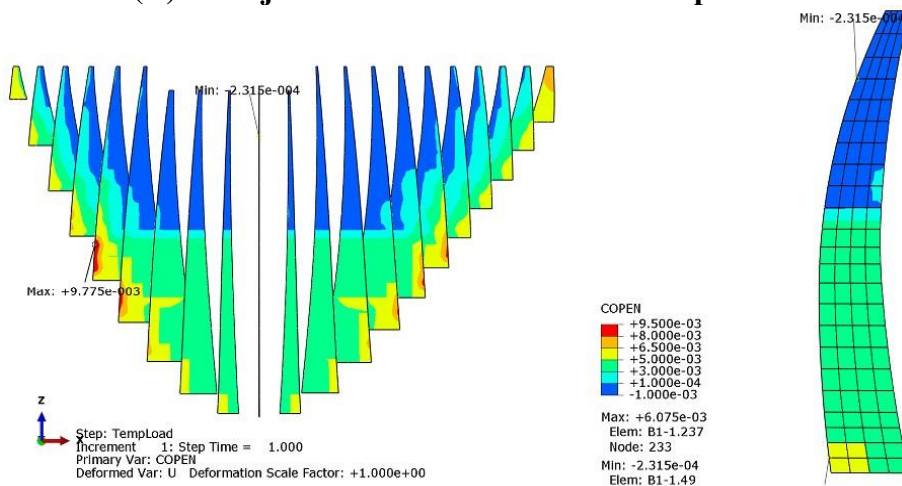
(B) No Injection from a Level of 915 m Upward

Figure 20. Joint Opening in m at a Normal Level and Under Winter-Time Thermal Loading in the Nonlinear Analysis and with no Injection in the Smooth Joint from Different Levels Upward with a Friction Coefficient of 1 and a Joint Thickness of 5 mm

Figure 21. Joint Opening in m at a Normal Level and Under Winter-Time Thermal Loading in the Nonlinear Analysis and with Full Injection in the Smooth Joint with a Joint Thickness of 1 mm
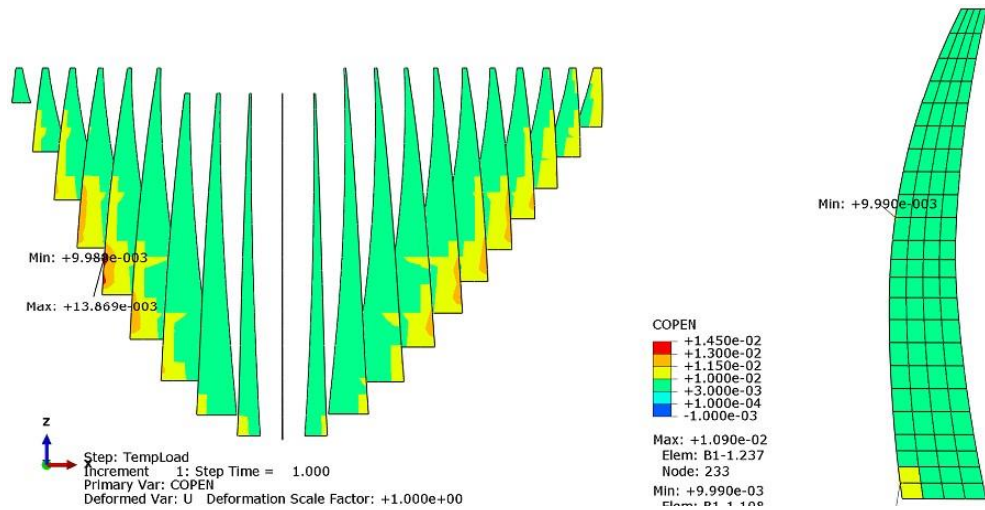

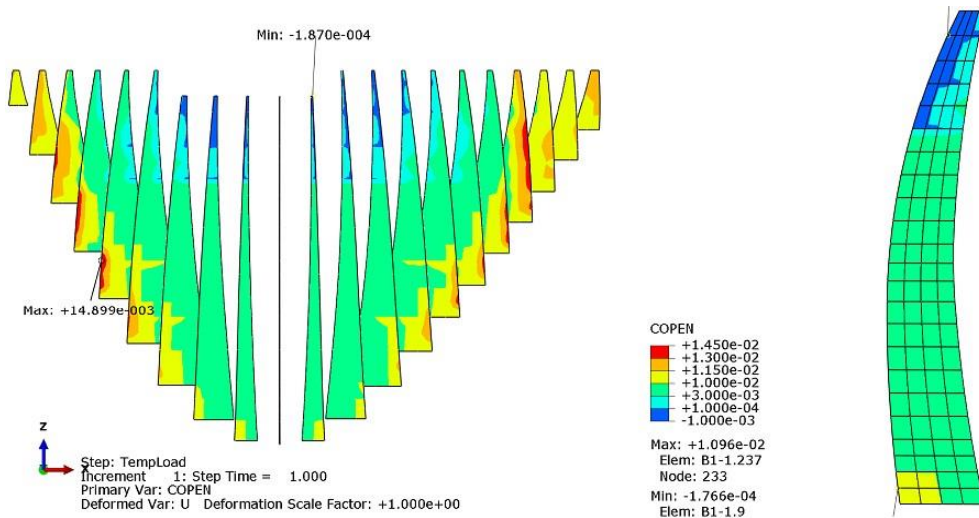**(A) No Injection from a Level of 955 m Upward**
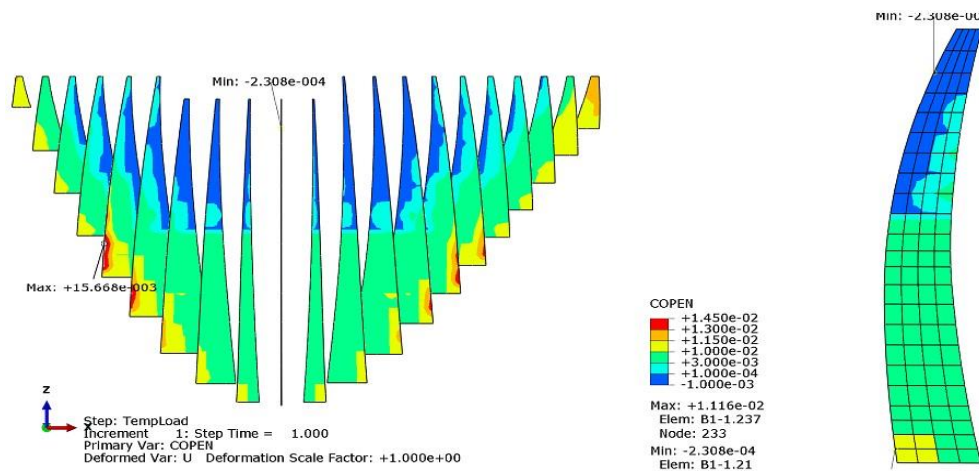

(B) No Injection from a Level of 915 m Upward

Figure 22. Joint Opening in m at a Normal Level and Under Winter-Time Thermal Loading in the Nonlinear Analysis and with no Injection in the Smooth Joint from Different Levels Upward with a Friction Coefficient of 1 and a Joint Thickness of 1 cm

As seen in the figures, the changes in the opening of the contraction joints were similar as the joint thickness increased, and only the relative opening of the joints increased .The largest value occurred at a joint with a thickness of 1 mm and at a maximum injection height of 915 m, indicating a 1.4 mm increase in the opening near the abutment compared to an initial thickness of 3 mm. Due to the large distance between the monolith at a maximum injection height of 955 m and a joint thickness of 1 cm, most of the monolith in the upper part did not come into contact. On the other hand, for the no-injection case with an initial thickness of 3 mm and a maximum injection height of 955 m, most of the upper monolith, and for a joint with an initial thickness of 5 mm, the middle monolith came into contact at the end of the loading.

4. Conclusion

Due to the complexity of the arched concrete dam structure, the design of this type of structure requires high experience and knowledge [25, 26]. The present research analyzed three numerical models with the aim of investigating the possible effect of incomplete injection in the contraction joints on double-curvature arch dams under hydrostatic loads. These models consist of a linear, integrated, and homogeneous model and two nonlinear models considering the nonlinear behavior resulting from two different types of common contraction joints in the dam's body. The obtained results can be summarized as follows:

1. The lack of injection led to a significant increase in the maximum principal stresses at the upstream section of the dam, such that a large part of this section, which originally worked under compression, is now under tension. The tensile stresses at the upstream abutment and the downstream crest also increased.

2. Under no injection conditions, the minimum principal stresses at the crest were reduced while the compressive stresses at the downstream abutment and downstream and upstream of the middle of the dam body increased.

3. With no injection into the contraction joints, the dam displacements significantly increased. Specifically, the displacements of the crest doubled for a joint without shear keys. However, the displacements further increased with a rise in the maximum injection height.

4. A lack of injection considerably increased the vertical compressive stresses between the contact surfaces. These stresses were increased almost twofold near the injection stop level. For example, the stresses between monolith zero and one increased from a maximum of 5.13 under complete injection to 11.3.

5. The results indicate that even with full injection in the contraction joints, openings can occur on the surfaces of these joints, mostly near the foundation. A lack of injection increases these openings although by a smaller amount compared to full injection. The amount of opening in the surfaces between the end monolith also increases, being higher in joints with shear keys than those without.

6. According to the results, with an increase in the joint thickness under the absence of joint injection, considerable amounts are added to the maximum principal stresses, minimum principal stresses, dam displacement, and the vertical compressive force between the contact surfaces.

7. As a general conclusion, the lack of injection at the upper surfaces of the dam does not significantly undermine the safety of the dam under static loads in case the incomplete injection height and the joint thickness are small. However, when the height of incomplete injection and the distance between the adjacent monolith increase, the dam may be at risk against static loads. Hence, sufficient attention must be paid to the injection of contraction joints in arch dams.

20

5. Refrences

1. Gu, C., Zhu, M., Wu, Y., Chen, B., Zhou, F., & Chen, W. (2023). Multi-output displacement health monitoring model for concrete gravity dam in severely cold region based on clustering of measured dam temperature field. *Structural Health Monitoring*, 14759217221142006.

2. Qin, X., Gu, C., Guo, J., Yuan, D., Shao, C., & Chen, X. (2023, January). Load combination feedback of fracture in concrete dams based on monitoring data with simplified fuzzy association rules. In *Structures* (Vol. 47, pp. 2354-2364). Elsevier.

3. Ouzandja, D., Messaad, M., Berrabah, A. T., & Belhrizi, M. (2023). Impact of material nonlinearity of dam-foundation rock system on seismic performance of concrete gravity dams. *Journal of Theoretical and Applied Mechanics*, 49-63.

4. Chen, C., & Chen, R. (2023). Application of magnesium oxide expansive agent in hydraulic concrete in China. *Magazine of Concrete Research*, 75(2), 97-106.

5. Ya, S., Eisenträger, S., Qu, Y., Zhang, J., Kuen, T., & Song, C. (2023). Seismic analysis of post-tensioned concrete gravity dams using scaled boundary finite elements implemented as ABAQUS UEL. *Soil Dynamics and Earthquake Engineering*, 164, 107620.

6. Tolstikov, V., & Youssef, Y. W. (2023). Impact of Joint Quality on Stress–Strain State and Stability of Bureyskaya Concrete Dam. In *Proceedings of FORM 2022* (pp. 371-382). Springer, Cham.

7. Wang, F., Song, Z., Liu, Y., & Li, C. (2023). Response characteristics and tensile failure evaluation of asphalt concrete core wall under spatial oblique incidence of P-wave. *Engineering Structures*, 276, 115340.

8. Wang, G., Shu, Y., Lu, W., Chen, M., Pan, X., & Lu, A. (2023). Damage prediction of concrete gravity dams subjected to penetration explosion. *Engineering Failure Analysis*, 143, 106855.

9. Guo, Y., Chen, X., Wang, Z., Ning, Y., & Bai, L. (2023). Identification of mixed mode damage types on rock-concrete interface under cyclic loading. *International Journal of Fatigue*, 166, 107273.

10. Krutov, D. A. (2023). Effectiveness Assessment of a Technique for Dam Reinforcement. *Power Technology and Engineering*, 1-6.

11. Zhao, X., Zhang, H., Wang, P., Ren, Q., Zhang, D., Yan, L., & Zhu, X. (2023). Flow-field fitting method applied to the detection of leakages in the concrete gravity dam. *Journal of Applied Geophysics*, 208, 104896.

12. Cacciuttolo, C., Pastor, A., Valderrama, P., & Atencio, E. (2023). Process Water Management and Seepage Control in Tailings Storage Facilities: Engineered Environmental Solutions Applied in Chile and Peru. *Water*, 15(1), 196.

13. Zhao, X., Tian, Y., Zhou, J., & Chai, Z. (2023). Experimental investigation on the effect of high-pressure water on tensile strength and microstructure of cementitious materials. *Construction and Building Materials*, 364, 129932.

14. Khafagy, A. (2023). The Concrete Function of the Banking System: Samir Amin's Monetary Theory of Financial Underdevelopment. *Available at SSRN 4317363*.

15. Liu, K., Guo, T., Yang, J., & Ma, S. (2023). Static and dynamic fracture behavior of rock-concrete bi-material disc with different interface crack inclinations. *Theoretical and Applied Fracture Mechanics*, 123, 103659.

16. Abrishami, J., Wahab Rajaei, N. (2010), Concrete dams design and construction. Fourth edition of Mashhad: Astan Quds Razavi Publications.

17. Chuhan, Z., Jianwen, P. & Jinting, W. (2009), "Influence of Seismic Input Mechanisms and Radiation Damping on Arch Dam Response", Soil Dynamics and Earthquake Engineering, Volume 29, pp. 1282-1283.

18. Yao, X. W., Elnashai, A. S. & Jiang, J. Q. (2012), "Analytical Seismic Fragility Analysis of Concrete Arch Dams", 15 WCEE, Lisboa.

19. Hariri-Ardebili, M. A., Mirzabozorg, H. & Kianoush, M. R. (2013), "Seismic Analysis of High Arch Dams Considering Contraction-Peripheral Joints Couplcd Effects", Central European Journal of Engineering, 3(3), pp. 549-564.

20. Ferdowsi et al. (2011), "The effect of accurate modeling of rock support sections of arched dams on the interactive behavior of the reservoir dam system", 10th Iran Hydraulic Conference, November, University of Guilan, Rasht,Iran

21. Ahmadi, M. T., Ahmadi, T. (2012), "Analysis of concrete arch dam failure with large displacements", 9th International Congress of Civil Engineering, May 19-21, Isfahan University of Technology, Isfahan.

22. Iran Water and Power Resources Development Company. (2004), "Final Stage Studies (Second Stage), Report on Supplementary Analysis of Dam Body and Abutments

23. Jenabi Dehkordi, A. (2011), "The effect of executive joints on the seismic behavior of arched concrete dams", Master Thesis, Urmia University.

24. Mahab Ghods Consulting Engineering Company. (2011), "Precision tools and behavior of Karun 4 dam and power plant", Report No. 33.

25. Pourbakhshian, S., & Ghaemian, M. (2015). Investigating stage construction in high concrete arch dams. *Indian Journal of Science and Technology*, *8*(14), 1.

26. Pouraminian, M., & Ghaemian, M. (2017). Multi-criteria optimization of concrete arch dams. *Scientia Iranica*, *24*(4), 1810-1820.